ACS APPLIED MATERIALS & INTERFACES

Research Article

www.acsami.org

Creating Water Vapor Barrier Coatings from Hydrophilic Components

Gerald Findenig,[†] Simon Leimgruber,[†] Rupert Kargl,*[,†] Stefan Spirk,[‡] Karin Stana-Kleinschek,[‡,§] and Volker Ribitsch[†,§]

[†]Division of Surface and Interface Science, Institute of Chemistry, Karl-Franzens-University Graz, Heinrichstraße 28, A-8010 Graz

[‡]Laboratory for Characterization and Processing of Polymers, University of Maribor, Smetanova 17, 2000 Maribor, Slovenia

[§]European Polysaccharide Network of Excellence (EPNOE)

ABSTRACT: The preparation of water vapor barrier coatings composed of polyelectrolyte/clay multilayers using the layer-by-layer technique is reported. The suitability of different synthetic and renewable polyelectrolytes for the preparation of barrier coatings in combination with montmorillonite (MMT) platelets as well as the influence of the ionic strength and the number of bilayers on the coating performance was investigated. Highly hydrophilic and permeable cellulose films were used as substrate for determining the influence of the coatings on the water vapor transmission rate (WVTR). Improved barrier properties were realized by the use of polyethylene imine (PEI) or 2-hydroxy-3-trimethylammonium propyl chloride starch (HPMA starch) in combination with MMT. After the application of only 5 bilayers of PEI and MMT (thickness ~40 nm) on each side of the cellulose film, the WVTR was significantly reduced. By the deposition of 40 PEI/MMT bilayers, the WVTR transmission rate was reduced by 68%. However, HPMA starch containing coatings led to vapor transmission reduction of up to 32% at the same number of coating steps. A strong correlation between the barrier properties of the coatings and the layer thickness was observed. The barrier properties of the coatings could be increased using higher ionic strengths. These results represent unprecedented water vapor barrier properties for coatings prepared from hydrophilic materials.

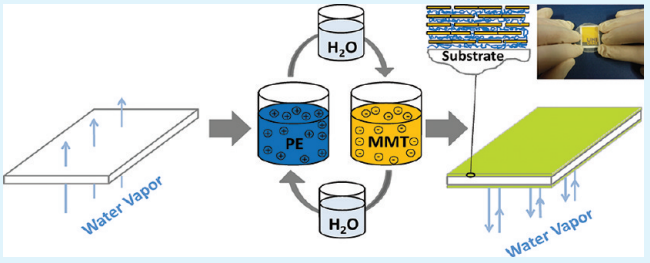

KEYWORDS: *water vapor barrier, layer-by-layer, montmorillonite, cellulose, polyelectrolyte, water vapor transmission*

INTRODUCTION

Barrier properties to gases, vapors, and flavors are one of the crucial requirements for many functional coatings and are therefore of particular technical and scientific interest.[1,2] Coatings with barrier properties are especially of importance in the field of packaging and electronics.[3−6] In addition to hydrophobic polymers, inorganic materials are used extensively for barrier coatings.[5] The high impermeability of these materials was already exploited in the built-up of multilayers from clay platelets and water-soluble polymers using the layer-by-layer (LbL) approach.[7,8] This method consists of the alternating deposition of positively and negatively charged components onto a solid substrate.[9,10] It offers the possibility to introduce a large variety of functional materials into a coating. This makes the technique a powerful tool to create customized barrier coatings. Nanometric LbL coatings on polyethylene terephthalate for instance, result in an excellent barrier for oxygen.[8,11] Recently, this approach was also used to increase the oxygen barrier properties of the biodegradable polymer polylactide (PLA).[12,13] These biodegradable polymers are of special interest, since many of them originate from renewable materials. However, a major drawback of many biopolymers is their sensitivity to humidity, which often limits their applicability. Cellulose films for example, show excellent oxygen barrier properties in the dry state but poor water vapor barrier properties due to the hydrophilic character of cellulose.[14] Under humid conditions, the excellent oxygen barrier properties of these films decrease significantly. To extend the applicability of biodegradable polymers, they are usually treated with top coatings of synthetic hydrophobic polymers.[15] While many polyelectrolytes are not fully biodegradable, their incorporation into a LbL barrier coating can represent a water-based ecologically friendly alternative. Even though LbL nanocomposites of polyelectrolytes and clays are known for their barrier to oxygen, their influence on the transmission of water vapor has not been studied extensively.

The aim of this work was therefore to study the formation of polyelectrolyte/clay multilayers on two types of substrates. For basic investigations in the film growth, the LbL films were prepared on silicon wafers and model films of cellulose. The model films were used to mimic the surface of commercial cellulose films. Cellulose was chosen as a representative biodegradable polymer with poor water vapor barrier properties. Coatings on these commercial films were characterized

Received: March 27, 2012
Accepted: May 31, 2012
Published: May 31, 2012

regarding their barrier to water vapor. The film growth of different synthetic and renewable polyelectrolytes in combination with montmorillonite (MMT) clay platelets was investigated. Polyethylene imine (PEI) and polydiallyldimethylammonium chloride (pDADMAC) were compared with chitosan and 2-hydroxy-3-trimethylammonium propyl chloride starch (HPMA starch). Additionally, the film forming behavior of the different polyelectrolytes in combination with the clay platelets was studied in dependence of the NaCl concentration since it is known that the multilayer build-up of polyelectrolytes can be influenced by the pH,[16−18] ionic strength,[16,19−22] and temperature.[23] Optical thickness and mechanical profilometry measurements were employed for the characterization of the thin coatings. Subsequently, the water vapor barrier properties of these multilayers were tested and related to their thickness and composition. A major target was to achieve the highest barrier with the lowest number of coating steps and to investigate the influence of the thickness and the coating composition on the barrier properties. This study should on the one hand elucidate details about the film formation and on the other hand allow the manufacturing of water vapor barriers coatings from hydrophilic components.

EXPERIMENTAL SECTION

Chemicals and Materials. Montmorillonite was provided by Rockwood Additives Ltd. (Widnes, UK). Aqueous MMT suspensions (0.1 wt %) in 18 MΩ cm Milli-Q water were prepared by rolling for 12 h. The insoluble components of the clay suspension were allowed to sediment for several hours. These components were removed by decanting. The sediment was dried and weighed (10% of the initial weight) and taken into account during the preparation of the MMT suspension in order to end up with the desired concentration of dispersed, nonsedimented clay. Branched polyethyleneimine (PEI) ($M_w \approx 25$ kDa), polydiallyldimethylammonium chloride (pDADMAC) (M_w = 200−350 kDa), and chitosan (low molecular weight; Brookfield viscosity = 20 Pa s) were purchased from Sigma-Aldrich (Austria) and used as received. HPMA starch (M_w = 1820 kDa, DS = 1.0) was synthesized as published elsewhere.[24] Figure 1 shows the structural formulas of the used polyelectrolytes (PE).

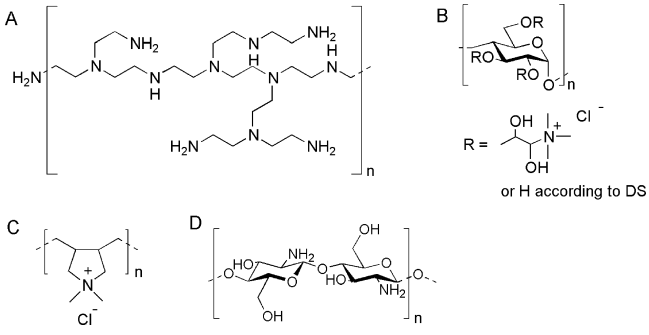

Figure 1. Chemical structure of the polyelectrolytes, (A) PEI, (B) HPMA starch, (C) pDADMAC, (D) and chitosan.

Polyelectrolyte solutions with a concentration of 0.1 wt % were prepared by shaking for 6 h and subsequent dissolution of the accordant amount of NaCl (30 mM and 500 mM). All polyelectrolyte solutions except those of chitosan were kept at their natural pH-values (10.3 for PEI, 4.9 for pDADMAC and 4.5 for HPMA starch). Chitosan was dissolved in Milli-Q-water at a pH of 3.5, adjusted with glacial acetic acid (Sigma-Aldrich). Pure cellulose films (21 μm thickness) and polyvinylidende chloride (PVDC) coated cellulose films were supplied by Innovia Films (Wigton, UK). Cellulose acetate (CA) films with a thickness of 25 μm were purchased from Goodfellow Ltd. (Bad Nauheim, Germany). Polyethylene terephthalat (PET) films (Mylar) with a thickness of 100 μm were purchased from DuPont. SiO_2 wafers (Silchem, Freiberg Germany) were cut into pieces of 1 × 4 cm^2 and cleaned by rinsing with Milli-Q water, acetone and again water. Afterward they were kept in piranha solution (70 vol. % conc. H_2SO_4 and 30 vol. % H_2O_2 (30 wt % in H_2O)) for 60 min. Finally the wafers were kept in water for 20 min, rinsed again with water and dried by a N_2-flow. Sarfus substrates with a SiO_2 surface were purchased from Nanolane (Montfort-le-Gesnois, France) and used as received.

Montmorillonite Platelet Characterization. The clay suspensions were characterized by photon correlation spectroscopy and zeta potential measurements using a Brookhaven Zeta Plus device (Holtsville, USA) equipped with a 35 mW solid state laser with a wavelength of 660 nm. Zeta potential measurements were performed using electrophoretic light scattering (ELS) in the phase analysis light scattering mode (PALS). A hydrodynamic diameter of 375 ± 6 nm and a zeta potential −52 ± 2 mV were found. The measurements were performed at a pH of 10, which represents the natural pH of a MMT suspension.

Model Film Preparation and LbL Coatings. Cellulose model films on Sarfus substrates (1 × 1 cm^2) were prepared by depositing 50 μL of a 1 wt % trimethylsilyl cellulose (TMSC) solution in toluene on the static substrate and subsequent spin coating (a: 2500 rpm s^{-1}, v: 4000 rpm, t: 60 s) with a Polos MCD wafer spinner (APT Ltd., Bienenbüttel, Germany) as described elsewhere.[25,26] The TMSC surfaces were regenerated by placing 2 mL hydrochloric acid (10 wt %) adjacent to the coated substrate in a Petri dish with 5 cm in diameter. The Petri dish was covered with its cap and the regeneration time was set to 10 min. The completeness of regeneration was followed by contact angle measurements and attenuated total reflectance infrared spectroscopy (ATR-IR) as described elsewhere.[27,28]

LbL films for the layer thickness determination on pure Sarfus substrates and cellulose thin film coated Sarfus substrates were prepared by alternating dipping of the substrate for ten minutes with the polyelectrolyte solution and MMT suspension, respectively. After each polyelectrolyte or clay coating, the films were thoroughly rinsed with Milli-Q water and dried in a stream of N_2 prior to film thickness determination.

For the preparation of the LbL films on silicon wafers and cellulose films, a home-build dip coating system was used. The cellulose films were cut into circular pieces with a diameter of 42 mm. Before fixation in circular frames they were preswollen in water. The films were subsequently dipped into the coating solutions (polyelectrolyte and MMT) for 10 min, starting with the polyelectrolyte solution. Each coating with polyelectrolyte or MMT was followed by an intermediate water dipping step for 10 min. The films were not dried between the single coating steps. All solutions were stirred during coating and washing. After finishing the coating procedure, the films were kept in the circular frames and dried under ambient conditions. Uncoated films were treated in the same way as coated films but dipped into solutions without polyelectrolyte and MMT. In order to simulate similar conditions as for the LbL coatings, the pH values and the ionic strength of the solutions were adjusted accordingly. All coatings in this work are denoted as $[\text{polyelectrolyte}_x/\text{MMT}]_y$, where y is the number of bilayers. One bilayer consists of one layer of polyelectrolyte and one layer of MMT. The subscript x describes the NaCl concentration of the polyelectrolyte solution in mM. The concentration of polyelectrolyte and MMT was 0.1 wt % for all experiments.

Film Thickness Measurements. The film thickness up to 5 bilayers was measured using the Sarfus technology (Nanolane, Montfort-le-Gesnois, France), which is based on the change of the polarization state of an incident linearly polarized light beam. For this technique special substrates, so-called Surfs are used, which do not alter the polarization state of an incident light beam and thus increase the contrast of the substrate. When a material is deposited on the substrate, the polarization of the reflected light beam is changed and is detected by cross polarized light microscopy. A more detailed description of this method can be found in literature.[29,30]

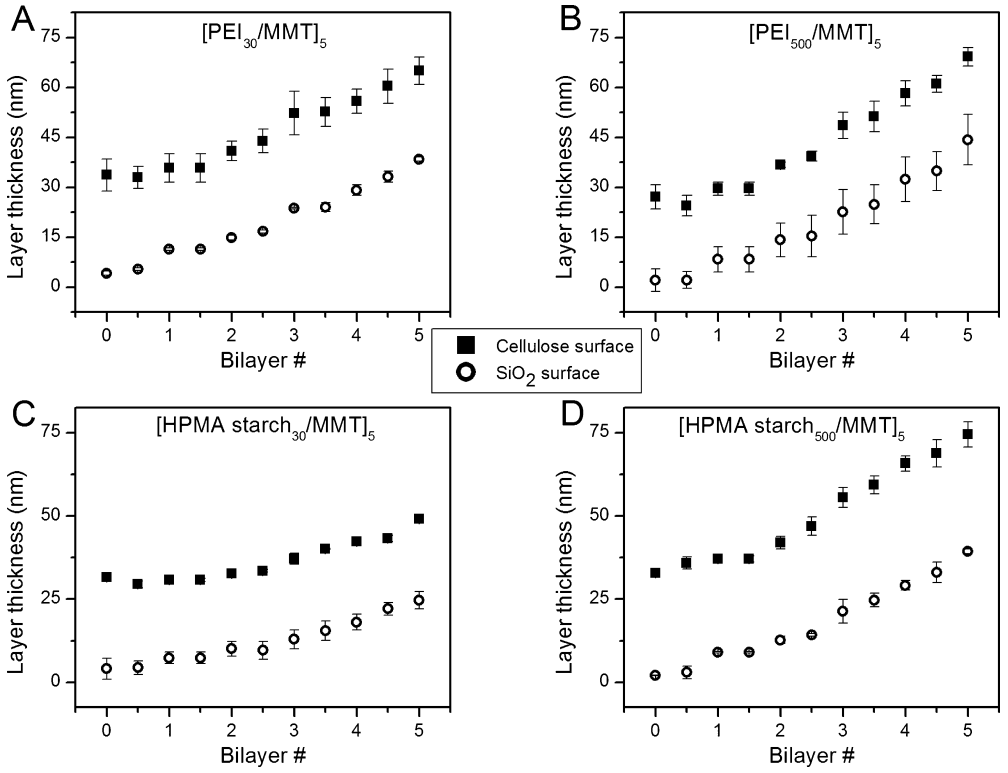

Figure 2. Film thickness growth functions of (A) $[PEI_{30}/MMT]_5$, (B) $[PEI_{500}/MMT]_5$, (C) $[HPMA\ starch_{500}/MMT]_5$, and (D) $[HPMA\ starch_{500}/MMT]_5$ coatings on cellulose and SiO_2 measured using the Sarfus technique.

The upper limit of the Sarfus calibration standard is 60 nm. Therefore profilometry was used to determine the thickness of coatings which exceeded 60 nm. All profilometry step height measurements were performed with coatings on SiO_2-wafers (1 × 4 cm^2). To create step heights, the coatings were partially removed using metal tweezers. For the profilometry measurements, a Dektak 150 surface profiler (Veeco instruments, Tucson, US) was used. The radius of the diamond tip was 12.5 μm and a stylus force of 3 mg was applied.

Atomic Force Microscopy and Mechanical Testing. The samples' surface morphology and roughness were determined using a Digital Instruments Dimension™ 3100 Scanning Probe Microscope (Digital Instruments Veeco Metrology Group, Plainview, NY, US) under ambient conditions. Intermittent contact mode images were collected using ultra sharp silicon cantilevers (OMCL-AC160TS-E, Atomic Force F&E GmbH, Mannheim, Germany) with a resonance frequency of 300 kHz and a force constant of 42 N m^{-1}. The root-mean-square surface roughness calculation and image processing were performed with the freeware Gwyddion (version 2.25).

The bursting strength of coated and uncoated films was determined using a Lorentzen & Wettre bursting strength tester (Stockholm, Sweden). A contact pressure of 460 kPa was used to fix the samples and each sample was measured 3 times.

Water Vapor Transmission Rate (WVTR) Measurements. The WVTR was measured using a self-made lab approach. Holes with a diameter of 32 mm were drilled into the screw caps of 100 mL glass bottles. Milli-Q-water (40 mL) was filled into the bottles. An O-ring was placed in the screw cap and the circular cellulose film (42 mm in diameter) was fixed with the screw cap on the bottle. The bottles were placed in a drying chamber at 35 °C. Uncoated cellulose films, which were dipped into solutions with adjusted pH and ionic strength, were used as reference. To keep the humidity in the drying chamber constant, we allowed air exchange with the ambient.

The relative humidity in the drying chamber was monitored by a capacitive humidity probe (Hygrosens Ltd., Donaueschingen, Germany) and never exceeded 25 ± 2%. During the measurement always 10 bottles were in the drying chamber. The weight loss of water over time was measured every 12 h using an analytical balance, with at least 4 measurement points per experiment. The WVTR in (g m^{-2} day^{-1}) was calculated according to eq 1. To allow a comparison of different experiments, all WVTR were normed to the WVTR of uncoated cellulose films, which did not deviate more than 5% in absolute values.

$$\text{WVTR (g m}^{-2}\text{ day}^{-1}\text{)} = \frac{\text{(initial mass (g) − mass after 24 h (g))}}{\text{area of the foil (m}^2\text{)}} \quad (1)$$

RESULTS AND DISCUSSION

Film Thickness Growth. The investigations on the coating thickness and film growth are a prerequisite for an efficient water vapor barrier since the thickness of the multilayer will obviously influence the coating performance. The multilayer build-up follows an almost linear function for all coatings during the first ten layers. Nevertheless differences in the growth functions between the cellulose model surface and the silicon dioxide surface can be observed. Figure 2 shows a comparison of the film growth functions with respect to the used polyelectrolyte, ionic strength and substrate. As an example PEI and HPMA starch were coated on two different substrates: pure silicon dioxide surfaces and cellulose model films.

For the experiments performed on cellulose model surfaces, the starting layer thickness is 30 nm, which represents the thickness of the initial cellulose layer. The growth follows in all cases an almost linear function, but there are minor differences depending on the used substrate. On silicon dioxide, the slope of the growth functions is constant over the whole number of bilayers. The growth functions of the coatings performed on cellulose in contrast, reveal two areas with slightly different slopes. The film thickness growth is less pronounced for the first two bilayers compared to the following three bilayers.

From our point of view two effects can be responsible for these observations. During the first adsorption steps, a penetration of the coating components into the cellulose film can occur. Second, the roughness of the cellulose film (rms 1.14 nm), in comparison to the silicon dioxide surface (rms 0.24 nm) could make the measurement technique insensitive to thickness changes of the first adsorbed layers.

Furthermore, the film thickness growth depends on the used ionic strength of the polyelectrolyte solutions. The HPMA starch coatings show a stronger influence of the used ionic strength on the film growth compared to the PEI coatings, which leads to a steeper slope when a higher salt concentration is used. The influence of the ionic strength on the film growth of the PEI containing coatings was not that pronounced and only slightly steeper slopes are observed at higher salt concentrations. Interestingly, after 2 bilayers, the build-up of the coatings is independent of the used substrate, because the slopes are in all cases very similar. This result is valuable, because theses coatings could also be used for other purposes on a variety of materials. The film growth of the other polyelectrolytes also follows a linear function and is independent of the substrate. Here again, the layer thickness is strongly correlated with the ionic strength and the type of polyelectrolyte. Figure 3 shows a comparison of the influence of

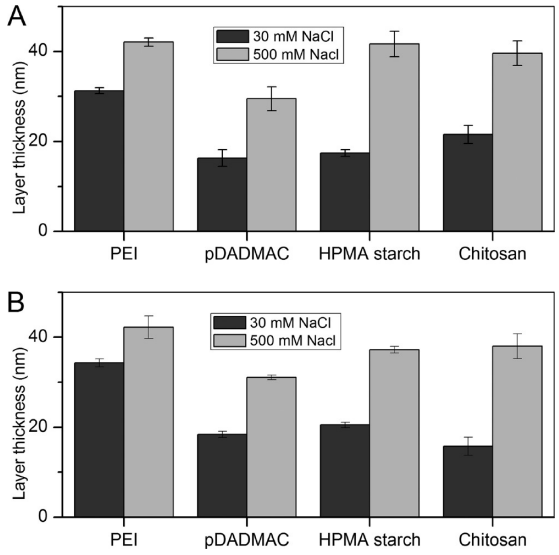

Figure 3. Influence of the ionic strength on the layer thickness of different polyelectrolyte/clay systems (5 bilayers). The coatings were prepared on (A) cellulose model films and (B) SiO_2.

the ionic strength on the final layer thickness of different polyelectrolyte/clay combinations on two different substrates (cellulose and SiO_2). The film thickness growth rate is independent whether cellulose (Figure 3A) or SiO_2 surfaces (Figure 3B) are coated. Even though there are slight differences in the absolute values of film thickness, the tendency of film formation and the influence of varying ionic strength is the same on both substrates.

In all cases, the film thickness of 5 bilayers increases with increasing ionic strengths. As known from other authors, this can be explained by a change in the conformation and solubility of the adsorbed polyelectrolyte.[16] Most polyelectrolytes adopt a densely packed structure at higher ionic strengths since intra- and intermolecular electrostatic repulsion is screened efficiently. Higher amounts of polyelectrolyte are deposited when the molecules can adsorb in a denser conformation. This should generally result in thicker layers at higher ionic strengths. PEI is used at its native pH of 10, where it is not fully charged and it already adopts a coiled structure without the addition of salt. This results in minor differences in the ionic strength dependent thickness of thin PEI films. PEI and chitosan are in contrast to pDADMAC and HPMA starch weak polyelectrolytes. The influence of varying ionic strengths on the film thickness is therefore less pronounced. Even though chitosan can also be considered as a weak polyelectrolyte, it is protonated at the given pH of 3.5. As a result, there are only minor differences in the film forming behavior between chitosan and strong polyelectrolytes.[16]

The nature and amount of the polyelectrolyte also influences the amount of deposited clay within the films. Larger amounts of deposited polyelectrolyte lead most likely to increased clay depositions. This can also be concluded from Figure 2 where both, clay and polyelectrolyte steps are increased concomitantly. The interaction of MMT with positively charged polyelectrolytes is governed by electrostatic and dispersive forces. Electrostatic interactions do not play the major role in the built up of the coatings since thicker layers are obtained at higher ionic strength where electrostatic forces are more and more screened. However the stability of the adsorbed polyelectrolyte will strongly depend on electrostatic interaction at decreased ionic strength after rinsing with water.

Investigations on the coating thickness at low numbers of bilayers give insights into differences of the used polyelectrolytes. Nevertheless for an increased coating thickness the film forming behavior can be very different and other influences than the polyelectrolyte structure gain importance. From literature, different shapes of growth functions of such multilayers, depending on the composition and the coating conditions, are known. The slope can be linear, exponential or even linear with two areas of different slopes.[16,18,31] To cover a wide range of thickness measurements, bilayer numbers of 5 to 40 were investigated with mechanical profilometry. PEI and HPMA starch were chosen for a more detailed characterization, because they lead, in contrast to chitosan and pDADMAC, to better barrier properties. Figure 4 shows a comparison of the film growth of PEI and HPMA starch coatings in combination with MMT at two ionic strengths on SiO_2.

Profilometry and Sarfus measurements of 5 bilayer coatings are comparable on both substrates. Since Sarfus measurements are limited to a layer thickness of 60 nm, thicker coatings were investigated using profilometry. At higher numbers of bilayers (10−40), PEI/MMT coatings reveal a minor influence of the ionic strength on the film thickness. For HPMA starch coatings the influence of the ionic strength on the film thickness of 5 bilayer films is not continued at 15 and 20 bilayers and only less pronounced at 30 and 40 bilayers. It has to be considered that at a high coating thickness, other effects than the polymer structure come into play. At higher bilayer numbers the surface roughness is increased and as a consequence more material can be deposited. Furthermore, heterogeneously deposited components can influence the overall amount of adsorbed material.

A strong influence on the growth rate of PEI/MMT and HPMA starch/MMT can be expected from the differences in molecular weight. The low molecular weight of PEI ($M_w \approx 25$ kDa) compared to HPMA starch($M_w = 1820$ kDa) can cause a higher penetration of PEI into the coating.

As a consequence, thicker coatings are obtained from PEI/MMT systems than for HPMA starch/MMT systems. The

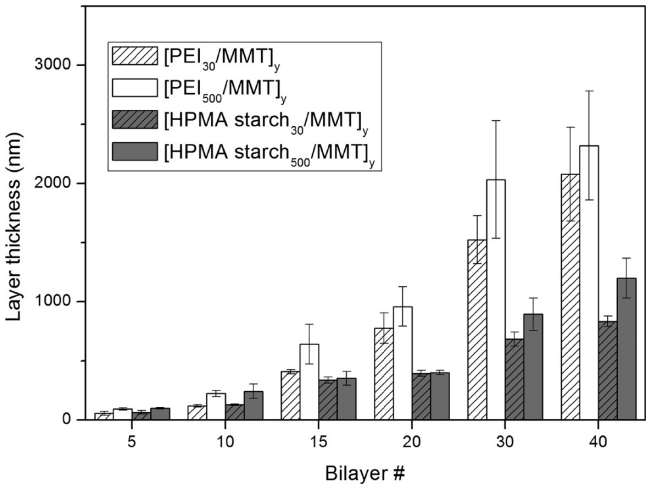

Figure 4. Film thickness growth of PEI and HPMA starch at two different ionic strengths (30 mM and 500 mM NaCl) in combination with MMT on SiO_2 substrates.

investigations on the coating thickness can be seen as a basis for the following WVTR measurements because the thickness will obviously influence the coating performance. Within the next sections, the WVTR of different coatings is therefore compared with their composition and thickness.

Water Vapor Transmission Rate Measurements. *Influence of the Type of Polyelectrolyte.* Several types of polyelectrolyte clay coatings have been characterized for their capability in the build-up of multilayers and subsequently a screening of their water vapor barrier properties has been performed. The aim was to investigate the influence of the type of polyelectrolyte on the WVTR and to exclude coatings with the lowest barrier. For that purpose, 40 bilayer coatings (20 on each side) of PEI, pDADMAC, HPMA starch, and chitosan in combination with MMT were applied on cellulose films. For all samples, the sodium chloride concentration in the polyelectrolyte solution was kept at 500 mM and 0.1 wt % MMT and polymer were used (Figure 5).

These experiments reveal that the coatings containing PEI provide barrier properties at a reasonable number of bilayers. An important reason for the observed effects is the coating thickness. Obviously, coatings with an increased thickness have improved barrier properties. Especially the system PEI/MMT shows a better performance than the other polyelectrolytes. The use of HPMA starch does also improve the barrier at 2 × 20 bilayers, whereas the coatings containing pDADMAC and chitosan lead only to small barrier improvements. For that reason the WVTR of coatings containing PEI and HPMA starch are investigated in detail within the next sections.

Detailed Barrier Properties of PEI/MMT and HPMA Starch/MMT Coatings. Figure 6 shows the WVTR and thickness of PEI/MMT and HPMA starch/MMT coatings prepared at two different ionic strengths (30 mM and 500 mM NaCl). As expected, the WVTR decreases with a higher number of bilayers for both polyelectrolytes.

As was shown in the previous section, the PEI/MMT coatings lead to the strongest barrier improvement. By applying 40 bilayers on each side of the substrate the transmission rate is reduced by 68% at a NaCl concentration of 30 mM. The WVTR decreases almost linearly with the number of bilayers. A coating of 5 bilayers on each side ($2[PEI_{30}/MMT]_5$) already reduces the WVTR by 22% (from 360 to 279 g m^{-2} day^{-1}). An increase of the bilayer numbers to 2 × 20 and 2 × 40 leads to reductions of 44% and 68%, respectively when PEI at 30 mM NaCl is used.

At higher ionic strengths (500 mM NaCl) thicker layers are formed, which leads to increased barrier properties of the films (24% at 2 × 5 and 62% at 2 × 20 applied bilayers). However, the formation of a stable 2 × 40 bilayer coating is not possible, because these coatings become too thick in the wet state and already adsorbed material is removed from the surface. This is

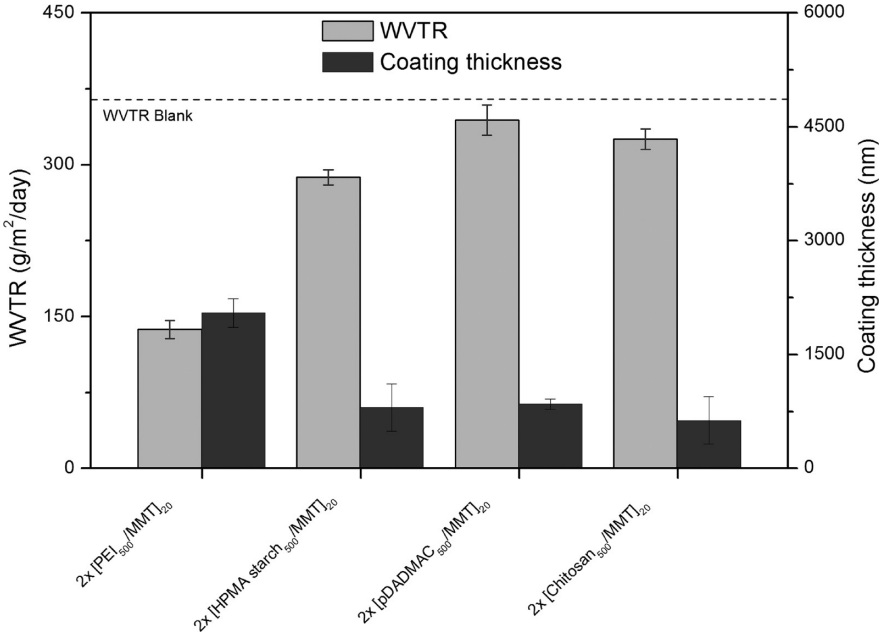

Figure 5. Influence of different polyelectrolytes on the water vapor barrier properties of commercial cellulose films. The water vapor transmission rates and thickness of 2 × 20 bilayer coatings containing PEI, pDADMAC, HPMA starch and chitosan are compared. The dashed line indicates the WVTR of the uncoated cellulose film.

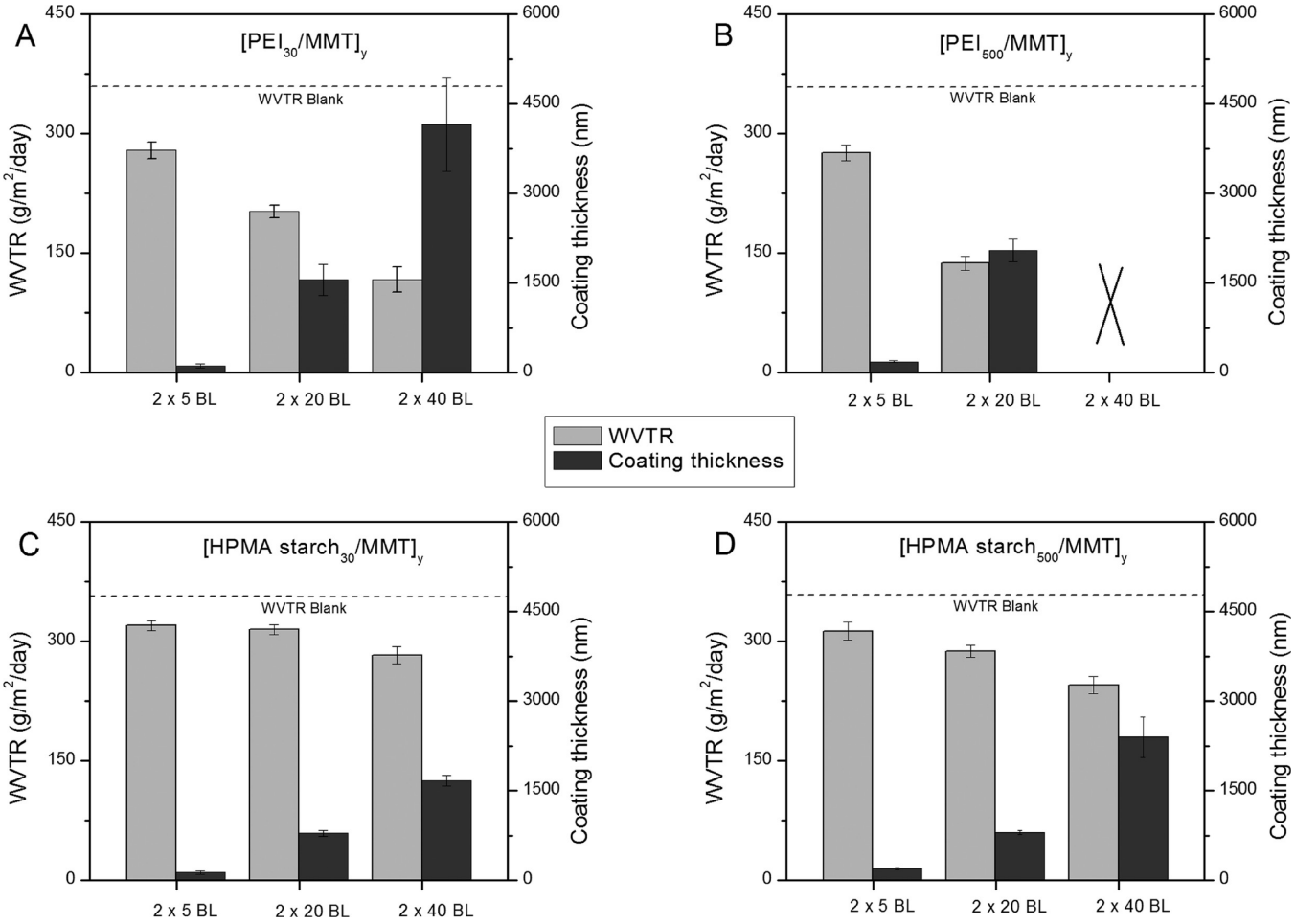

Figure 6. Water vapor transmission rate and thickness of (A) $[PEI_{30}/MMT]_y$, (B) $[PEI_{500}/MMT]_y$, (C) $[HPMA\ starch_{30}/MMT]_y$, and (D) $[HPMA\ starch_{500}/MMT]_y$ coatings with different numbers of bilayers. The dashed lines indicate the WVTR of the uncoated cellulose film.

only the case for the $2[PEI_{500}/MMT]_{40}$ coating. In general, higher salt concentrations of the polyelectrolyte solution lead to better barrier properties because of a larger amount of adsorbed material and therefore thicker layers. Additionally it seems that after a certain number of bilayers more adsorbed material does not lead to a corresponding barrier improvement, since the barrier properties of the coatings $2[PEI_{500}/MMT]_{20}$ and $2[PEI_{30}/MMT]_{40}$ are similar but they show a difference in layer thickness. A possible explanation for this phenomenon is that the coating is not well-structured after a certain bilayer number.

In general, it is known that polyelectrolyte/MMT multilayers reduce the permeability for gases such as oxygen.[8,12] Nevertheless, the water vapor barrier properties of coatings prepared from aqueous solutions on a hydrophilic substrate are unprecedented. Although a higher number of bilayers is necessary to provide acceptable barrier properties, a significant effect on the transmission can already be observed at a coating thickness of 40 nm on each side of the cellulose substrate.

The HPMA starch/MMT coatings are in general thinner than the PEI/MMT coatings. This is also reflected in the barrier properties, since the highest achieved barrier reductions with a starch containing coating is 32% ($2[HPMA\ starch_{500}/MMT]_{40}$). Nevertheless, besides the film thickness, the composition of the coatings is another important factor. 2 × 5 bilayer coatings of PEI/MMT reveal almost the same thickness as HPMA starch/MMT coatings, but they show better barrier properties. In contrast to PEI, HPMA starch contains hydroxyl and quarternary ammonium groups, which causes a higher hydrophilicty of the incorporated polymer backbone. As a result, the affinity of the coating toward water is increased and swelling might be more pronounced.

As already shown and discussed in the previous sections, electrolytes can be added to influence the thickness of the multilayers. Thus, also the WVTR can be influenced by the concentration of salt at the same number of coating steps. Obviously, better barrier properties are obtained at increased ionic strengths, which is a result of the increased coating thickness. If one compares PEI and HPMA multilayers, the barrier properties of coatings with the same thickness differ significantly. This can be attributed to the aforementioned structural differences of the polyelectrolytes composing the films. More hydrophilic polyelectrolytes seem to reduce the barrier against water vapor.

The requirements to obtain an effective water vapor barrier are therefore a high concentration of densely packed clay, which is strongly held together by a polyelectrolyte with a relatively hydrophobic backbone. With the measurement method used in this study a maximum barrier improvement of 68% was determined. For comparative reasons the WVTR of commercially available coatings and other packaging materials was determined with the same method. Cellulose films coated with polyvinylidene chloride (6 g/(m^2 day) and 98% reduction compared to pure cellulose), cellulose acetate films (14 g/(m^2

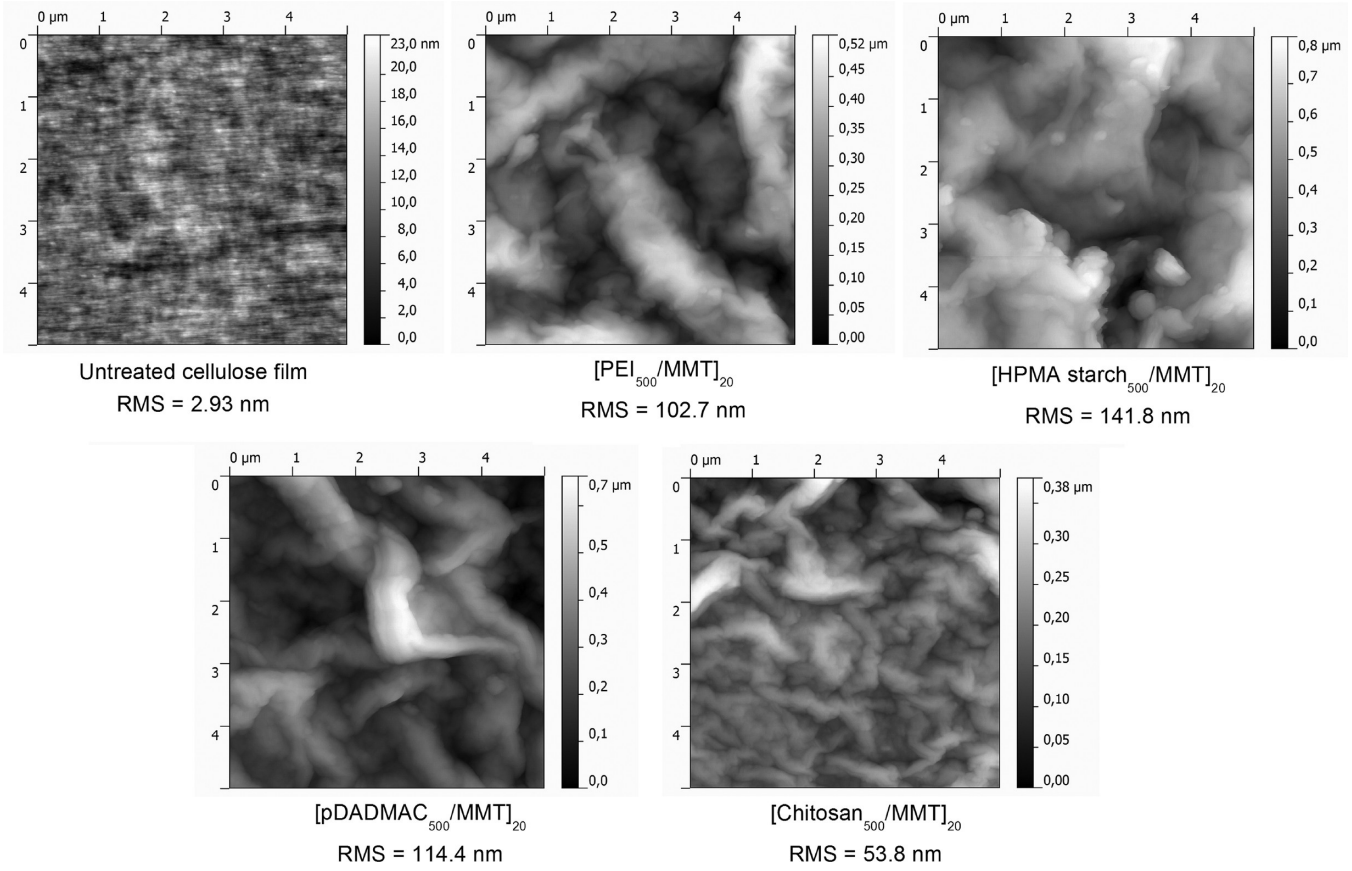

Figure 7. AFM surface morphology of an untreated cellulose film and different 20 bilayer coatings.

day) and 95% reduction) and PET films (4 g/(m^2 day) and 99% reduction) are superior to the coatings elaborated in this work. Nevertheless it was successfully shown that it is possible to prepare water vapor barrier coatings using hydrophilic components. The performance of these coatings can further be improved by variation of coating parameters and applied components.

Characterization of the Surface Morphology and Transparency. The surface morphology of [polyelectrolyte$_{500}$/MMT]$_{20}$ coatings was investigated using AFM in tapping mode. Figure 7 shows topography images of an untreated cellulose film and of polyelectrolyte/clay coated films. The surface roughness (rms roughness) of the samples is depicted below each image.

The surface of an untreated cellulose film is smooth (rms = 2.93 nm) and shows a fibrillar surface texture, which originates from the manufacturing process of the films. The coated films reveal very different surface features and much higher roughness values. Even though it is difficult to discern quantitative differences from the AFM measurements, chitosan/MMT multilayers can be qualitatively distinguished from the other coatings. All surfaces exhibit a relatively dense structure of clay, but PEI and HPMA starch coatings give the densest morphology. Even the clay coatings with higher numbers of bilayers show high transparency (Figure 8), which is also independent of the used polyelectrolyte when the same coating thickness is applied. This is especially advantageous for an application on transparent packaging materials.

From a qualitative point of view the LbL coatings are stable and do not peel off when the cellulose substrates are bent.

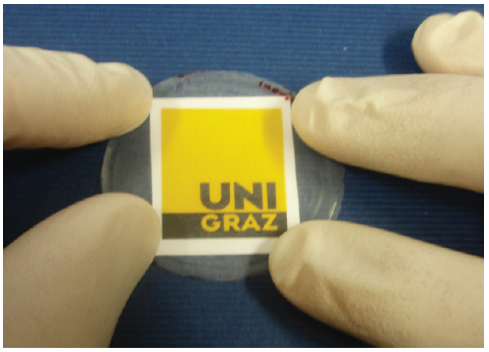

Figure 8. Image of a cellulose film with a 2[PEI$_{30}$/MMT]$_{20}$ coating.

Simple scratching with for instance plastic tweezers cannot abrade the coatings. Quantitatively we determined the bursting strength of 2 × 20 bilayer coatings containing HPMA starch and PEI (each at 500 mM salt). We found a 10% increase in bursting strength for both coatings. Pure cellulose films reveal a bursting strength of 413 ± 23 kPa, whereas PEI containing coatings give 471 ± 6 kPa and HPMA starch containing coatings 452 ± 21 kPa. It can be concluded, that the LbL coatings applied in this work improve other relevant material properties such as the bursting strength. Further experiments to elaborate the influence of LbL coatings on the mechanical properties of the substrate would therefore be of interest.

CONCLUSION

In this paper, the successful layer-by-layer preparation of water vapor barrier coatings from aqueous solutions and hydrophilic

dx.doi.org/10.1021/am300542h | ACS Appl. Mater. Interfaces 2012, 4, 3199−3206

components on highly permeable cellulose films was demonstrated. This procedure provides an ecologically friendly coating process to create barrier materials. To prepare polyelectrolyte/clay multilayers, the layer-by-layer approach was chosen, where the polyelectrolytes act as mortar and the montmorillonite (MMT) platelets act as impermeable bricks. Four different types of polyelectrolytes/MMT coatings were characterized and compared with respect to their barrier properties against water vapor. Optical layer thickness measurements revealed an almost linear growth function for all polyelectrolyte clay combinations at low numbers of coating steps. In contrast, mechanical profilometry measurements showed differences in the growth rate of thicker coatings. PEI/MMT formed thicker coatings than HPMA starch/MMT at the same number of bilayers.

Polyethyleneimine (PEI) and 2-hydroxy-3-trimethylammonium propyl chloride starch (HPMA starch) turned out to be suitable for the preparation of barrier coatings with a reasonable number of coating steps and the barrier properties correlated well with the layer thickness. The layer thickness and therefore the barrier properties were increased with higher ionic strength of the polyelectrolyte solution. Nonetheless also the type of polyelectrolyte influenced the barrier properties. PEI/MMT layers of the same thickness were superior to HPMA starch/MMT coatings, which can most likely be attributed to differences in hydrophilicty of the polymer backbone. All coatings lead to transparent layers, which are applicable for a great variety of materials. The preparation of water vapor barriers from hydrophilic materials using the LbL approach is therefore a promising tool in materials science and technology.

AUTHOR INFORMATION

Corresponding Author

*E-mail: rupert.kargl@uni-graz.at. Phone: 0043 316 380 5413. Fax: 0043 316 380 9850.

Notes

The authors declare no competing financial interest.

ACKNOWLEDGMENTS

Prof. Thomas Heinze from the University of Jena is highly acknowledged for providing the TMSC and HPMA starch. The research leading to these results has received funding from the European Union Seventh Framework Programme (FP7/2007-2013) under Grant 214653.

REFERENCES

(1) Kim, J.-K.; Hu, C.; Woo, R. S. C.; Sham, M.-L. *Compos. Sci. Technol.* **2005**, *65*, 805−813.
(2) Chatham, H. *Surf. Coat. Technol.* **1996**, *78*, 1−9.
(3) Sanchez-Garcia, M. D.; Lopez-Rubio, A.; Lagaron, J. M. *Trends Food Sci. Technol.* **2010**, *21*, 528−536.
(4) Sanchez-Garcia, M. D.; Lagaron, J. M. *J. Appl. Polym. Sci.* **2010**, *118*, 188−199.
(5) Langereis, E.; Creatore, M.; Heil, S. B. S.; Van De Sanden, M. C. M.; Kessels, W. M. M. *Appl. Phys. Lett.* **2006**, 89 art. no. 081915..
(6) Jung, K.; Bae, J.-Y.; Park, S. J.; Yoo, S.; Bae, B.-S. *J. Mater. Chem.* **2011**, *21*, 1977−1983.
(7) Jang, W.-S.; Rawson, I.; Grunlan, J. C. *Thin Solid Films* **2008**, *516*, 4819−4825.
(8) Priolo, M. A.; Gamboa, D.; Grunlan, J. C. *ACS Appl. Mater. Interfaces* **2010**, *2*, 312−320.
(9) Decher, G.; Hong, J. D.; Schmitt, J. *Thin Solid Films* **1992**, *210*−*211*, 831−835.
(10) Decher, G. *Science* **1997**, *277*, 1232−1237.
(11) Priolo, M. A.; Gamboa, D.; Holder, K. M.; Grunlan, J. C. *Nano Lett.* **2010**, *10*, 4970−4974.
(12) Svagan, A. J.; Åkesson, A.; Cárdenas, M.; Bulut, S.; Knudsen, J. C.; Risbo, J.; Plackett, D. *Biomacromolecules* **2012**, *13*, 397−405.
(13) Laufer, G.; Kirkland, C.; Cain, A. A.; Grunlan, J. C. *ACS Appl. Mater. Interfaces* **2012**, *4*, 1643−1649.
(14) Crouzier, T.; Boudou, T.; Picart, C. *Curr. Opin. Colloid Interface Sci.* **2010**, *15*, 417−426.
(15) Plackett, D. In *Biopolymers−New Materials for Sustainable Films and Coatings*, 1st ed.; John Wiley and Sons: UK, 2011; pp 85−90.
(16) Lundin, M.; Solaqa, F.; Thormann, E.; Macakova, L.; Blomberg, E. *Langmuir* **2011**, *27*, 7537−7548.
(17) Shiratori, S. S.; Rubner, M. F. *Macromolecules* **2000**, *33*, 4213−4219.
(18) Elzbieciak, M.; Zapotoczny, S.; Nowak, P.; Krastev, R.; Nowakowska, M.; Warszyński, P. *Langmuir* **2009**, *25*, 3255−3259.
(19) Buron, C. C.; Filiâtre, C.; Membrey, F.; Bainier, C.; Buisson, L.; Charraut, D.; Foissy, A. *Thin Solid Films* **2009**, *517*, 2611−2617.
(20) Rojas, O. J.; Claesson, P. M.; Muller, D.; Neuman, R. D. *J. Colloid Interface Sci.* **1998**, *205*, 77−88.
(21) Dubas, S. T.; Schlenoff, J. B. *Langmuir* **2001**, *17*, 7725−7727.
(22) McAloney, R. A.; Dudnik, V.; Goh, M. C. *Langmuir* **2003**, *19*, 3947−3952.
(23) Chang, L.; Kong, X.; Wang, F.; Wang, L.; Shen, J. *Thin Solid Films* **2008**, *516*, 2125−2129.
(24) Haack, V.; Heinze, T.; Oelmeyer, G.; Kulicke, W.-M. *Macromol. Mater. Eng.* **2002**, *287*, 495−502.
(25) Schaub, M.; Wenz, G.; Wegner, G.; Stein, A.; Klemm, D. *Adv. Mater.* **1993**, *5*, 919−922.
(26) Kontturi, E.; Thüne, P. C.; Niemantsverdriet, J. W. *Langmuir* **2003**, *19*, 5735−5741.
(27) Mohan, T.; Kargl, R.; Doliška, A.; Vesel, A.; Köstler, S.; Ribitsch, V.; Stana-Kleinschek, K. *J. Colloid Interface Sci.* **2011**, *358*, 604−610.
(28) Mohan, T.; Kargl, R.; Doliška, A.; Ehmann, H. M. A.; Ribitsch, V.; Stana-Kleinschek, K. *Carbohydr. Polym.* **2012**, DOI: 10.1016/j.carbpol.2012.02.033.
(29) Ausserré, D.; Valignat, M.-P. *Opt. Express* **2007**, *15*, 8329−8339.
(30) Ausserré, D.; Valignat, M.-P. *Nano Lett.* **2006**, *6*, 1384−1388.
(31) Yang, Y.-H.; Haile, M.; Park, Y. T.; Malek, F. A.; Grunlan, J. C. *Macromolecules* **2011**, *44*, 1450−1459.